

# EFFECT OF A REALISTIC THREE-BODY FORCE ON THE ENERGY SPECTRA OF ${}_{\Lambda}^{13}\text{C}$ , ${}_{\Lambda}^{17}\text{O}$ , ${}_{\Lambda}^{40}\text{K}$ AND ${}_{\Lambda}^{48}\text{K}^*$

J. POKORNÝ<sup>a</sup>, G. DE GREGORIO<sup>b,c</sup>, F. KNAPP<sup>d</sup>, N. LO IUDICE<sup>c,e</sup>  
P. VESELÝ<sup>b</sup>

<sup>a</sup>Faculty of Nuclear Sciences and Physical Engineering  
Czech Technical University in Prague, 115 19 Prague, Czech Republic

<sup>b</sup>Nuclear Physics Institute, Czech Academy of Sciences  
250 68 Řež, Czech Republic

<sup>c</sup>INFN Sezione di Napoli, Naples, Italy

<sup>d</sup>Faculty of Mathematics and Physics, Charles University, Prague, Czech Republic

<sup>e</sup>Dipartimento di Fisica, Università di Napoli Federico II, Naples, Italy

(Received January 7, 2019)

We adopt the Hartree–Fock (HF) method and the nucleon– $\Lambda$  Tamm–Dancoff Approximation (NA TDA) to study the energy spectra of selected medium mass hypernuclei composed of a  $\Lambda$  hyperon bound to an even–even and odd–even nuclear cores. Our calculations are carried out using the  $YN$  LO potential plus the chiral potential  $\text{NNLO}_{\text{sat}}$ , which includes explicitly the 3-body  $NNN$  force. This component, while improving the r.m.s. radii of the nuclear cores and the relative distances between levels or group of levels of the hypernuclear spectra, strongly reduces the binding energies indicating that the inclusion of more complex configurations is badly needed.

DOI:10.5506/APhysPolBSupp.12.657

## 1. Introduction

The theoretical study of medium-mass and heavy hypernuclei may provide a guide for a better understanding of the hyperon–nucleon ( $YN$ ) interaction at momentum scales not accessible in few-body systems.

Several methods, based mostly on phenomenological potentials, have been developed for this purpose. We mention the Skyrme Hartree–Fock model [1–3] and the relativistic mean field (RMF) model [4, 5].

---

\* Presented at the XXV Nuclear Physics Workshop “Structure and Dynamics of Atomic Nuclei”, Kazimierz Dolny, Poland, September 25–30, 2018.

We started a project whose objective is to provide an *ab initio* description of medium-mass and heavy hypernuclei starting from modern realistic nucleon–nucleon and baryon–nucleon potentials, and to go beyond mean field by studying the role of complex many-body configurations. This final goal will eventually be reached by resorting to the Equation of Motion Phonon Method (EMPM). This method has been developed for nuclear structure studies [6] and extensively adopted for light and heavy even–even [7–10] and medium-mass odd–even nuclei [11–13].

The preliminary step of our approach consists in developing the Hartree–Fock (HF) method in the proton–neutron– $\Lambda$  ( $p$ – $n$ – $\Lambda$ ) scheme and, then, the nucleon– $\Lambda$  Tamm–Dancoff Approximation (NA TDA) formalism. HF is suited for describing hypernuclei with one  $\Lambda$  particle bound to an even–even nuclear cores, while NA TDA allows us to study hypernuclei consisting of one  $\Lambda$  coupled to an odd–even nuclear cores [14].

Here, we have adopted the two methods to study the effect of the  $NNN$  part of the chiral  $NNLO_{\text{sat}}$  potential [15] on selected nuclei and hypernuclei. In particular, we compute the r.m.s. radii and binding energies of  $^{12}\text{C}$ ,  $^{16}\text{O}$ ,  $^{40}\text{Ca}$  and  $^{48}\text{Ca}$ , the single-particle energies of  $\Lambda$  in  $^{13}\text{C}$  and  $^{17}\text{O}$  and the energy spectra of  $^{40}\text{K}$  and  $^{48}\text{K}$ .

We do not take into account the effect of the  $\Lambda$ – $\Sigma$  mixing. This issue is discussed in the conclusions.

## 2. Theoretical formalism

We adopted the intrinsic Hamiltonian

$$H = T + V^{NN} + V^{NNN} + V^{N\Lambda} - T_{\text{CM}}, \quad (1)$$

where  $T$  is the kinetic energy operator of nucleons and  $\Lambda$ ,  $T_{\text{CM}}$  is the centre-of-mass kinetic operator, and  $V^{NN}$ ,  $V^{N\Lambda}$ , and  $V^{NNN}$  stand for the 2-body  $NN$ , the  $N\Lambda$ , and the 3-body  $NNN$  potentials, respectively.

The HF equations are

$$\begin{aligned} t_{ij}^p + \sum_{kl} V_{ikjl}^{pp} \rho_{lk}^p + \sum_{kl} V_{ikjl}^{pn} \rho_{lk}^n + \sum_{kl} V_{ikjl}^{p\Lambda} \rho_{lk}^\Lambda + \frac{1}{2} \sum_{klmn} V_{ikljmn}^{ppp} \rho_{mk}^p \rho_{nl}^p \\ + \frac{1}{2} \sum_{klmn} V_{ikljmn}^{ppn} \rho_{mk}^p \rho_{nl}^n + \sum_{klmn} V_{ikljmn}^{ppn} \rho_{mk}^p \rho_{nl}^n = \varepsilon_i^p \delta_{ij}, \end{aligned} \quad (2)$$

$$\begin{aligned} t_{ij}^n + \sum_{kl} V_{ikjl}^{nn} \rho_{lk}^n + \sum_{kl} V_{kilj}^{pn} \rho_{lk}^p + \sum_{kl} V_{ikjl}^{n\Lambda} \rho_{lk}^\Lambda + \frac{1}{2} \sum_{klmn} V_{ikljmn}^{nnn} \rho_{mk}^n \rho_{nl}^n \\ + \frac{1}{2} \sum_{klmn} V_{klimnj}^{ppn} \rho_{mk}^p \rho_{nl}^p + \sum_{klmn} V_{klimnj}^{ppn} \rho_{mk}^p \rho_{nl}^n = \varepsilon_i^n \delta_{ij}, \end{aligned} \quad (3)$$

$$t_{ij}^A + \sum_{kl} V_{kilj}^{pA} \rho_{lk}^p + \sum_{kl} V_{kilj}^{nA} \rho_{lk}^n = \varepsilon_i^A \delta_{ij}, \quad (4)$$

where  $\rho_{nm}^p$ ,  $\rho_{nm}^n$  and  $\rho_{nm}^A$  are the density matrices for protons, neutrons and  $\Lambda$ , respectively.

The solution of the HF equations gives the single-particle energies  $\varepsilon_i^p$ ,  $\varepsilon_i^n$  of the nucleons and yields the energies  $\varepsilon_i^A$  of the  $\Lambda$  hyperon bound to the even-even nuclear core [14].

The energy spectra of hypernuclei consisting of one  $\Lambda$  coupled to an odd-even nuclear cores are determined by solving the NA TDA eigenvalue equations. To this purpose, we solve separately the HF Eqs. (2)–(3) for the nucleons of the core and Eq. (4) for  $\Lambda$ . The energies and basis states so obtained enter the NA TDA eigenvalue equations

$$\sum_{ph} \left( (\varepsilon_p^A - \varepsilon_h^p) \delta_{pp'} \delta_{hh'} - V_{\bar{h}p'\bar{h}'p}^{pA} \right) r_{ph}^{\mu,pA} = (E_\nu^{pA} - E_{\text{HF}}) r_{p'h'}^{\mu,pA}, \quad (5)$$

$$\sum_{ph} \left( (\varepsilon_p^A - \varepsilon_h^n) \delta_{pp'} \delta_{hh'} - V_{\bar{h}p'\bar{h}'p}^{nA} \right) r_{ph}^{\mu,nA} = (E_\nu^{nA} - E_{\text{HF}}) r_{p'h'}^{\mu,nA}. \quad (6)$$

### 3. Calculation details and results

We have solved the HF equations starting from the harmonic oscillator (HO) basis with  $\hbar\omega = 16$  MeV. As shown in Ref. [14], the convergence is satisfactory if we include all two-body and three-body matrix elements under the restrictions  $\{ij\} : 2n_i + l_i + 2n_j + l_j \leq N_{\text{max}}\}$  and  $\{ijk\} : 2n_i + l_i + 2n_j + l_j + 2n_k + l_k \leq N_{\text{max}}\}$ , with  $N_{\text{max}} = 12$ .

#### 3.1. HF calculation of $^{12}\text{C}$ , $^{16}\text{O}$ , $^{40}\text{Ca}$ and $^{48}\text{Ca}$ nuclear cores

The charge radii and binding energies of  $^{12}\text{C}$ ,  $^{16}\text{O}$ ,  $^{40}\text{Ca}$  and  $^{48}\text{Ca}$  are calculated by solving the HF Eqs. (2)–(3) for nucleons only ( $\rho^A = 0$ ). These equations have been solved with and without the  $NNN$  component of the  $\text{NNLO}_{\text{sat}}$  potential [15].

The mean-square charged radius is given by

$$\langle r_{\text{ch}}^2 \rangle = \left( 1 - \frac{1}{A} \right) \frac{1}{Z} \langle r_p^2 \rangle + R_p^2 + \frac{N}{Z} R_n^2 + \frac{3\hbar^2}{4m_p^2 c^2}, \quad (7)$$

where  $\langle r_p^2 \rangle = \int dr r^4 \rho_p(r)$  is the mean-square proton point radius,  $R_p = 0.8775(51)$  fm,  $R_n^2 = -0.1149(27)$  fm<sup>2</sup>, and  $\frac{3\hbar^2}{4m_p^2 c^2} = 0.033$  fm<sup>2</sup> [15].

As shown in Table I, the charge radii  $r_{\text{ch}}$  calculated with the 2-body  $NN$  interaction only are too small. They are enhanced once the  $NNN$  force is included, in much better agreement with the experiments.

TABLE I

The charge radii  $r_{\text{ch}} = \sqrt{\langle r_{\text{ch}}^2 \rangle}$  [fm] and binding energies  $\text{BE}/A$  [MeV] of  $^{12}\text{C}$ ,  $^{16}\text{O}$ ,  $^{40}\text{Ca}$  and  $^{48}\text{Ca}$  calculated with  $NN$  and  $NN + NNN$  forces are compared with the experimental data (exp.) [18].

${}^A X$	$NN$	$NN + NNN$	exp.
$r_{\text{ch}}$			
$^{12}\text{C}$	2.13	2.52	2.47
$^{16}\text{O}$	2.19	2.77	2.70
$^{40}\text{Ca}$	2.58	3.54	3.48
$^{48}\text{Ca}$	2.55	3.57	3.47
$\text{BE}/A$			
$^{12}\text{C}$	4.59	1.70	7.68
$^{16}\text{O}$	7.36	2.66	7.98
$^{40}\text{Ca}$	11.65	2.31	8.55
$^{48}\text{Ca}$	12.95	1.93	8.67

The effect of the 3-body  $NNN$  force on nuclear radii is caused by its repulsive character. This term, in fact, reduces strongly the binding energies of the nuclei under study (Table I), indicating that ground-state correlations are needed. The strong impact on the physical observables induced by more complex configurations emerges from the calculations using the  $\text{NNLO}_{\text{sat}}$  potential within a Coupled Cluster (CC) [15] and a SCGF approach [16].

The effect of the correlations has been also studied within the EMPM using the  $\text{NNLO}_{\text{opt}}$  potential [17].

This calculation, while affecting weakly the charge radii, yielded a contribution to the binding energy coming from two-phonon correlations comparable to the HF contribution.

On the ground of this EMPM calculation and the results obtained in Refs. [15, 16] with  $\text{NNLO}_{\text{sat}}$ , we expect that the ground-state correlations estimated within the EMPM should counterbalance the contribution coming from the strongly repulsive  $NNN$  part of the  $\text{NNLO}_{\text{sat}}$  potential, thereby filling to a large extent the gap with experiments.

### 3.2. Energy spectra of ${}_{\Lambda}^{13}\text{C}$ , ${}_{\Lambda}^{17}\text{O}$ , ${}_{\Lambda}^{40}\text{K}$ and ${}_{\Lambda}^{48}\text{K}$ hypernuclei

The hypernuclear energy spectra are calculated adopting the  $NA-NA$  channel of the chiral  $YN$  LO potential [19] with the regulator cut-off parameter  $\lambda = 550$  MeV which yields for the hypernuclei under study binding energies of  $\Lambda$  closer to the empirical values.

The hypernuclear energy spectra depend almost linearly on  $\lambda$  for the employed  $YN$  LO potential [14]. Therefore, the relative distances among the energy levels are marginally affected by this parameter.

The  $NNN$  force affects strongly the single-particle levels of  $\Lambda$  in  ${}^{13}_{\Lambda}\text{C}$  and  ${}^{17}_{\Lambda}\text{O}$  (Fig. 1). In fact, the energy gaps are significantly reduced once the  $NNN$  force is included. The relative distances among the  $s$ -,  $p$ - and  $sd$ -major shells get closer to the empirical levels.

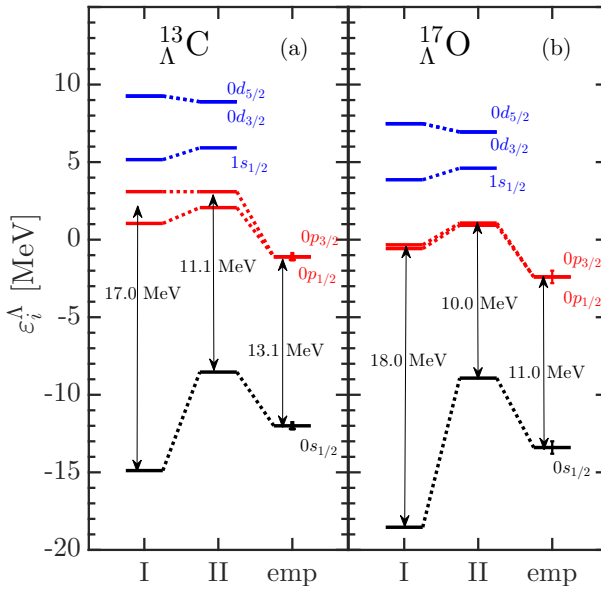


Fig. 1. The  $\Lambda$  single-particle energies  $\varepsilon_i^{\Lambda}$  in  ${}^{13}_{\Lambda}\text{C}$  (a) and in  ${}^{17}_{\Lambda}\text{O}$  (b) calculated with  $NN$  (I) and  $NN + NNN$  (II) interactions. The empirical energies (emp.) interpreted from the experimental measurements [20] are shown for comparison.

However, the calculated energy spectra are shifted upward in energy with respect to the experimental data. This clearly indicates that the correlations induced by more complex configurations are needed.

The too large splitting between  $0p_{1/2}$  and  $0p_{3/2}$  levels, especially in  ${}^{13}_{\Lambda}\text{C}$ , may be reduced by including the  $\Lambda$ - $\Sigma$  mixing in the  $YN$  interaction not taken into account in the present calculation.

The  $NNN$  force affects strongly the spectra of  ${}^{40}_{\Lambda}\text{K}$  and  ${}^{48}_{\Lambda}\text{K}$ . As shown in Fig. 2, the  $NA$  TDA calculation yields multiplets of states which are far apart from each other when only the  $NN$  is used. The separations between these multiplets are drastically reduced by the  $NNN$  force.

Unfortunately, there are no experimental data for these two hypernuclei. An experiment for their production is planned at JLab [21]. Once more complex configurations are included through the EMPM, our calculations will provide the hypernuclear wave functions needed for the theoretical analysis of the data.

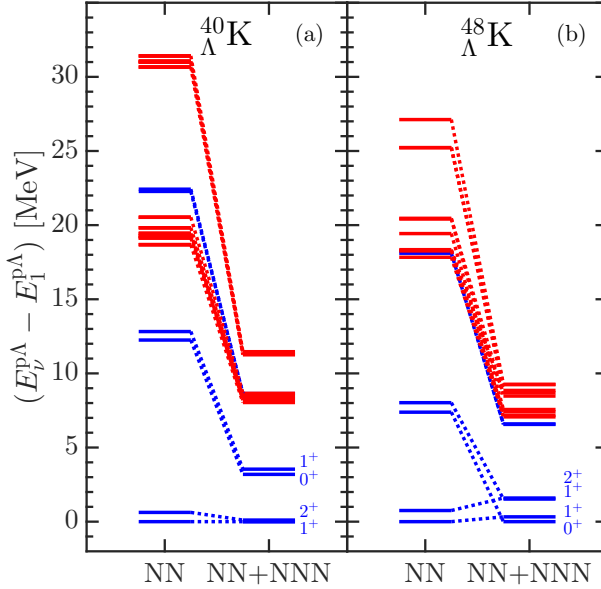


Fig. 2. (Colour on-line) The relative energies of  ${}_{\Lambda}^{40}\text{K}$  (a) and  ${}_{\Lambda}^{48}\text{K}$  (b) calculated with  $NN$ , and  $NN + NNN$  forces. The grey/red (black/blue) lines represent the states with the negative (positive) parity.

#### 4. Conclusions

The results presented here put in evidence the strong effect of the  $NNN$  component of the  $NNLO_{\text{sat}}$  potential on nuclei and hypernuclei. In nuclei, the charge radii of  ${}^{12}\text{C}$ ,  ${}^{16}\text{O}$ ,  ${}^{40}\text{Ca}$ ,  ${}^{48}\text{Ca}$  get close to the experimental values once the  $NNN$  force is included. Because of its repulsive nature, however, this force reduces considerably the  $NN$  contribution to the nuclear binding energies which are strongly underestimated.

The  $NNN$  force has a strong impact also on the hypernuclear energy spectra. It yields for  ${}^{13}_{\Lambda}\text{C}$  and  ${}^{17}_{\Lambda}\text{O}$   $\Lambda$  single-particle energy separations close to the empirical ones apart from an overall upward shift of the levels.

An analogous effect is also observed in the energy spectra of  ${}_{\Lambda}^{40}\text{K}$  and  ${}_{\Lambda}^{48}\text{K}$ . The  $NNN$  force reduces significantly the gaps among the multiplets of levels. Such an effect may be tested in planned future experiments.

In order to bridge the gap with the experimental nuclear binding energies and to reproduce the absolute energies of hypernuclei, it is necessary to include more complex excitations. This will be achieved by resorting to the EMPM.

The method derives and solves iteratively a set of equations of motion to generate an orthonormal basis of multiphonon states built of TDA phonons. Such a basis simplifies the structure of the Hamiltonian matrix and makes feasible its diagonalization in large configuration and phonon spaces. The diagonalization of the Hamiltonian in the multiphonon space so constructed produces highly correlated states, including the ground state. It takes into full account the Pauli principle and holds for any Hamiltonian.

We extend the method to hypernuclei with even–even and odd–even cores. In these two cases, we couple, respectively, the  $\Lambda$  states and the  $N\Lambda$  TDA phonons to the many particle–hole excitations of the nuclear cores.

Another important issue is the inclusion of the  $\Lambda$ – $\Sigma$  mixing in the  $YN$  LO interaction. We plan to include the  $N\Lambda$ – $N\Sigma$  part of the chiral LO  $YN$  interaction into the  $N\Lambda$ – $N\Lambda$  channel through the SRG transformation. Such a transformation has the effect of suppressing the  $\Lambda$ – $\Sigma$  mixing terms and generating thereby a 3-body  $YNN$  force to be added to the SRG transformed 2-body  $YN$  potential [22].

J. Pokorný acknowledges Czech Technical University SGS grant No. SGS16/243/OHK4/3T/14. Highly appreciated was the access to computing and storage facilities provided by the Meta Centrum under Program No. LM2010005 and the CERITSC under the program Centre CERIT Scientific Cloud, part of the Operational Program Research and Development for Innovations, Register No. CZ.1.05/3.2.00/08.0144.

## REFERENCES

- [1] H.-J. Schulze, E. Hiyama, *Phys. Rev. C* **90**, 047301 (2014).
- [2] M. Rayet, *Nucl. Phys. A* **367**, 381 (1981).
- [3] D.E. Lanskoy, Y. Yamamoto, *Phys. Rev. C* **55**, 2330 (1997).
- [4] J. Mareš, B.K. Jennings, *Nucl. Phys. A* **585**, 347 (1995).
- [5] B.-N. Lu, E. Hiyama, H. Sagawa, S.-G. Zhou, *Phys. Rev. C* **89**, 044307 (2014).
- [6] D. Bianco *et al.*, *Phys. Rev. C* **85**, 014313 (2012).
- [7] F. Knapp *et al.*, *Phys. Rev. C* **90**, 014310 (2014).
- [8] F. Knapp *et al.*, *Phys. Rev. C* **92**, 054315 (2015).
- [9] G. De Gregorio, F. Knapp, N. Lo Iudice, P. Veselý, *Phys. Rev. C* **93**, 044314 (2016).
- [10] G. De Gregorio, F. Knapp, N. Lo Iudice, P. Veselý, *Phys. Scr.* **92**, 074003 (2017).

- [11] G. De Gregorio, F. Knapp, N. Lo Iudice, P. Veselý, *Phys. Rev. C* **94**, 061301(R) (2016).
- [12] G. De Gregorio, F. Knapp, N. Lo Iudice, P. Veselý, *Phys. Rev. C* **95**, 034327 (2017).
- [13] G. De Gregorio, F. Knapp, N. Lo Iudice, P. Veselý, *Phys. Rev. C* **97**, 034311 (2018).
- [14] P. Veselý, G. De Gregorio, J. Pokorný, *Phys. Scr.* **94**, 014006 (2019) [arXiv:1811.00853 [nucl.th]].
- [15] A. Ekström *et al.*, *Phys. Rev. C* **91**, 051301(R) (2015).
- [16] T. Duguet *et al.*, *Phys. Rev. C* **95**, 034319 (2017).
- [17] G. De Gregorio *et al.*, *Phys. Rev. C* **95**, 024306 (2017).
- [18] I. Angeli, *At. Data Nucl. Data Tables* **87**, 185 (2004).
- [19] H. Polinder, J. Haidenbauer, U.-G. Meißner, *Nucl. Phys. A* **779**, 244 (2006).
- [20] A. Agnello *et al.*, *Phys. Lett. B* **698**, 219 (2011).
- [21] JLab Hypernuclear Collaboration, experiment E12-15-008, approved by JLab PAC44, 2016.
- [22] R. Wirth, R. Roth, *Phys. Rev. Lett.* **117**, 182501 (2016).